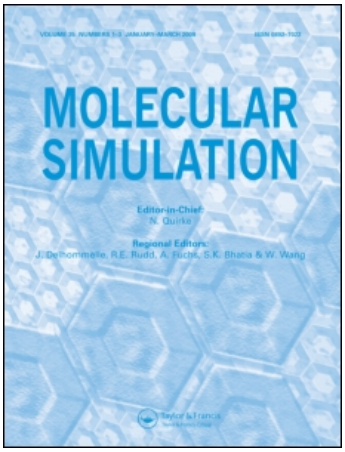

Molecular Simulation
Publication details, including instructions for authors and subscription information:
http://www.informaworld.com/smpp/title~content=t713644482

Molecular Simulation of Solution Conformations of the Amyloid β-Peptide Aβ(1-42) by a Backpropagation Neural Network Model

Peter P. Mager[a]
[a] Research Group of Pharmacochemistry, Institute of Pharmacology Toxicology of the University, Saxony, Germany

To cite this Article Mager, Peter P.(2001) 'Molecular Simulation of Solution Conformations of the Amyloid β-Peptide Aβ(1-42) by a Backpropagation Neural Network Model', Molecular Simulation, 27: 1, 43 — 59
To link to this Article: DOI: 10.1080/08927020108024518
URL: http://dx.doi.org/10.1080/08927020108024518

Molecular Simulation, 2001, Vol. 27, pp. 43–59
Reprints available directly from the publisher
Photocopying permitted by license only

MOLECULAR SIMULATION OF SOLUTION CONFORMATIONS OF THE AMYLOID β-PEPTIDE Aβ(1-42) BY A BACKPROPAGATION NEURAL NETWORK MODEL

PETER P. MAGER*

Research Group of Pharmacochemistry, Institute of Pharmacology and Toxicology of the University, D-04107 Leipzig, Härtelstr. 16-18, Saxony, Germany

(Received October 2000; accepted October 2000)

The predictive power of solution-dependent conformational states of the Aβ(1-42) peptide of Alzheimer' s disease by an optimized backpropagation neural network was tested. It was found that the neural network simulates well the solution-dependent conformations. The model was also examined by using geometry-optimized conformations (hybrid approach of Gasteiger charges plus MM+ molecular-mechanics) where the initial coordinates were obtained by NMR solution spectroscopy.

Keywords: Optimized backpropagation neural network; Circular dichroism spectra; Amyloid β-peptide; Alzheimer's disease; β-sheet; Conformation-dependent biological activity; Molecular modelling

INTRODUCTION

Alzheimer's disease (AD) is a chronic, neurodegenerative disorder which is characterized by pathological brain lesions composed of amyloid deposition [5, 6, 15, 17]. Extracellular deposits consist of amyloid plaques and cerebrovascular amyloid, while intracellular deposits consist of neurofibrillary tangles. The major protein constituent of the deposits is the so-called

*e-mail: magp@server3.medizin.uni-leipzig.de

amyloid β-peptide (Aβ) which is derived from proteolysis of a large (653 to 770 amino acids) transmembrane amyloid precursor protein (APP) by an endosomal/lysosomal processing pathway [9].

Several variants of the naturally occuring Aβ's differing only at the C-terminus (amino acid residues 1-39, 1-40, 1-42, 1-43) are formed by the proteolytic cleavage from the amyloid precursor protein. It appears that the Aβ(1-40) and Aβ(1-42) are the predominant proteins in neuritic plaque while Aβ(1-43) is present as a minor component, and Aβ(1-39) is a predominant component in cerebrovascular deposits [9, 14].

Furthermore, it was demonstrated that freshly prepared random-coil conformation of Aβ(1-40) and Aβ(1-42) is nontoxic or less toxic, while an enhanced neurotoxicity is observed after inducing an aging of a β-sheet conformation by a suitable chemical medium [18]. The finding that a biological activity depends on protein conformation, and that conformational transitions generate new biological properties, is also of interest in understanding the role of other proteins (such as viral proteins).

Unfortunately, experimental studies in peptide research have been suffering if the concentrations reach a critical limit [10, 20]. The ability of cascading β-sheets to form highly aggregates renders studies on conformation conversions experimentally very difficult, as also shown by investigating experimentally and theoretically other, more simple peptide models [7, 8]. While it is relatively easy to work experimentally with Aβ(1-40), the longer peptide Aβ(1-42) aggregates more easily. This implies that it is hard to assess chemical purity of Aβ(1-42) above the 70% level [20]. Furthermore, although it is well documented that a protein's folded tertiary structure is encoded by its amino acid sequence, the conformation of proteins is formed along a relatively unknown, "largely mysterious", folding pathways.

Consequently, experimentally based conformation analysis of the Aβ(1-42) peptide is difficult, and it should be useful to predict solution conformations of the Aβ(1-42) peptide. As theoretical method, neural networks were applied because they have become powerful tools to mimic problems of functional relationships, frequently giving better results than conventional statistical approaches. Among the various neural network techniques, an optimized backpropagation neural network was chosen.

METHOD

The estimates of α-helix conformation of Aβ(1-42) were determined by circular dichroism (CD) spectra (units of deg·cm^2/decimol) at θ_{208}

where θ_{208} denotes the mean residue ellipticity at a wavelength of 208 nm. The β-sheet (y%) and random-coil conformation (z%) were determined by ordinary least-squares regression. The average error was error ± 10%. The conformations were determined in dependence on the peptide concentration, the concentration of the solvents trifluoroethanol (TFE) and hexafluoro-2-propanol (HFIP) that promote hydrogen-bonding forces, and the pH values. The data were taken from Barrow *et al.* [2] and are relisted in Table I. The β-turn structure was estimated by

TABLE I Solution conformations of the amyloid β-peptide Aβ(1-42) in dependence on the peptide concentration (Conc, μM), the concentration of trifluoroethanol (TFE) and hexafluoro-2-propanol (HFIP*) in water (% solv.), and the pH values. The effect of the adjusted percentages of the conformational states is denoted by # (to get 100%), it is less than the experimental error of ± 10%

Input data			*Output data (percentages)*			
Conc	*% solv.*	*pH*	*α-helix*	*β-sheet*	*Coil*	*β-turn*
9	0	2.8	0	86	14	0
9	10	2.8	0	88	12	0
9	15	2.8	0	95	5	0
9	20	2.8	20	45	31	4
9	30	2.8	44	5	26	25
9	40	2.8	39	2	29	30
9	60	2.8	35	13	30	22
9	90	2.8	40	0	21	39
10	0	7.3	0	79	21	0
10	10	7.3	0	83	17	0
10	15	7.3	0	75#	25	0
10	20	7.3	3	63	33	1
10	30	7.3	26	24	37	23
10	40	7.3	28	12	36	24
10	60	7.3	38	3	35	24
10	90	7.3	41	0	32	27
14	0	2.8	0	82	18	0
14	10*	2.8	24	55	21#	0
14	20*	2.8	41	22	33	4
14	30*	2.8	44	14	33	9
14	40*	2.8	44	10	32	14
14	60*	2.8	44	5	32	19
12	0	1.4	0	78	22	0
12	0	2.9	0	80	20	0
12	0	5.0	0	95	5	0
12	0	7.3	0	90	10	0
12	0	10.0	0	73	27	0
12	0	12.0	0	73	27	0
15	25	1.3	28	40	30	2
15	25	3.0	25	50	25#	0
15	25	5.5	0	80	10	10
15	25	7.6	23	50	25	2
15	25	8.3	28	40	32#	0
15	25	9.6	34	40	26#	0

$100\% - (x+y+z)\%$. From these percentages, spectra of a computer-assisted prediction of circular dichroism spectra [16] were determined and compared with the experimentally obtained data.

The algorithm of the backpropagation neural network was described elsewhere [22]. As model parameters, the following layers were used: (i) the input layer with linear transfer function and 3 nodes: peptide concentration conc (μM), the concentration (%) of the α-helix stabilizing agents TFE (trifluoroethanol) and HFIP (hexafluoro-2-propanol), and pH values; (ii) the first hidden layer with sigmoidal transfer function and 4 nodes; and (iii) the output layer with sigmoidal transfer function and 4 nodes (percentages of α-helix, β-sheet, random coil, and β-turn). All possible connections were analyzed. The sigmoidal backpropagation functions were solved by the nonlinear Levenberg-Marquardt algorithm. The learning rate *momentum* was equal to 0.8, the learning rate minimum and maximum were equal to 0.001 and 0.3, and the learning rate criterion was equal to 0.059. As goodness-of-fit criteria, the multivariate and squared multiple correlation coefficients (R^2) were used and statistically tested [11]. The software can be downloaded, address see end of the study. Optimization was achieved by (i) estimating the global error vector prior to adjusting weights, and (ii) updating successively the weights until convergence was reached.

The coordinates of the Aβ(1-40) peptide were generated from solution NMR data (25 degrees Celsius) and downloaded from the Brookhaven Protein Data Bank (1AML PDB file). Then, the two missing amino acids Ile41 and Ala42 were added by a sequence editor. As NMR spectroscopy may produce a considerable variability of bond lengths, bond angles, and torsion angles due to experimental errors, and the resulting structures may correspond to one of perhaps many low-energy conformations, geometry optimization was used to improve the geometry data and to get the most stable conformers. The conformations were initially energy minimized using the MM+ force field without an electrostatic term. The MM+ empirical potential (force field) is an improved MM2/MM3 version [1, 19]. The whole MM+ procedure was repeated with electrostatic parameters of the connectivity-based iterative partial equalization of orbital electronegativity [4]. After including the partial charges, the resulting conformation contained the molecular electrostatic potential and electrostatic energies. Correlation-gradient geometry optimization was then achieved [3]. The structures were refined using a conjugate gradient minimizer (Fletcher-Reeves modification of the Polak-Ribière method). Convergence was obtained when the gradient root mean square RMS was $RMS < 0.1$.

RESULTS AND DISCUSSION

Training Set of the Backpropagation Neural Network Model

The design matrix listed in Table I can be downloaded (address see end of this study), so that the reader can easily reexamine the calculations and results. Table II shows the major results. The squared multiple correlation coefficients R^2 are statistically tested by using the maximum-likelihood criterion Λ at the 5% significance level [11] using $p=4$ output nodes ("regressands") and $c=3$ input nodes ("regressors") with the sample size $N=34$. Each R^2 which is equal to or larger than $\Lambda=0.517$ is significant at the 5% level or less. The experimentally obtained and theoretically calculated percentages of the conformational states are illustrated in Figures 1–4, together with the 95% confidence and prediction limits. The number of potential outliers is relatively low (raw vectors 14 and 31 with respect to the α-helix, raw vector 3 with respect to the β-sheet, raw vectors 3 and 4 with respect to the random coil, raw vectors 7 and 31 with respect to the β-turn) and, more importantly, the deviations from the confidence bands are practically negligible compared with the experimental error rate ($\pm$ 10%). It is remarkable that the internal relationships between the input parameters are near-zero (the inflation factors are 0.03, 0.04 and 0.01). This shows clearly that the solution conditions influence independently the conformational states. Subsequent analysis led to the result that the most important factor is the solution effect of the solvents, followed by the peptide concentration.

Remarks Using the hyberbolic-tangent and hyperbolic-secant transfer functions of backpropagation, the goodness-of-fit criteria were less well (within the ranges 0.89 to 0.64 and 0.93 to 0.88, respectively). Using the radial-basis network approach and solving the Gaussian transfer function by thinplate-spline or multiquadratic (and inverse multiquadratic) methodology, even poorer results were found (within the range 0.68 to 0.41).

TABLE II Results of the training set using the complete number of sample members (SD = standard deviation)

Output node	*SD*	*Bias*	*Max. error*	R^2
α-helix	5.03	−0.19	13.21	0.956
β-sheet	6.00	0.12	16.02	0.983
Random coil	4.01	0.22	9.40	0.888
β-turn	3.78	−0.22	12.23	0.944

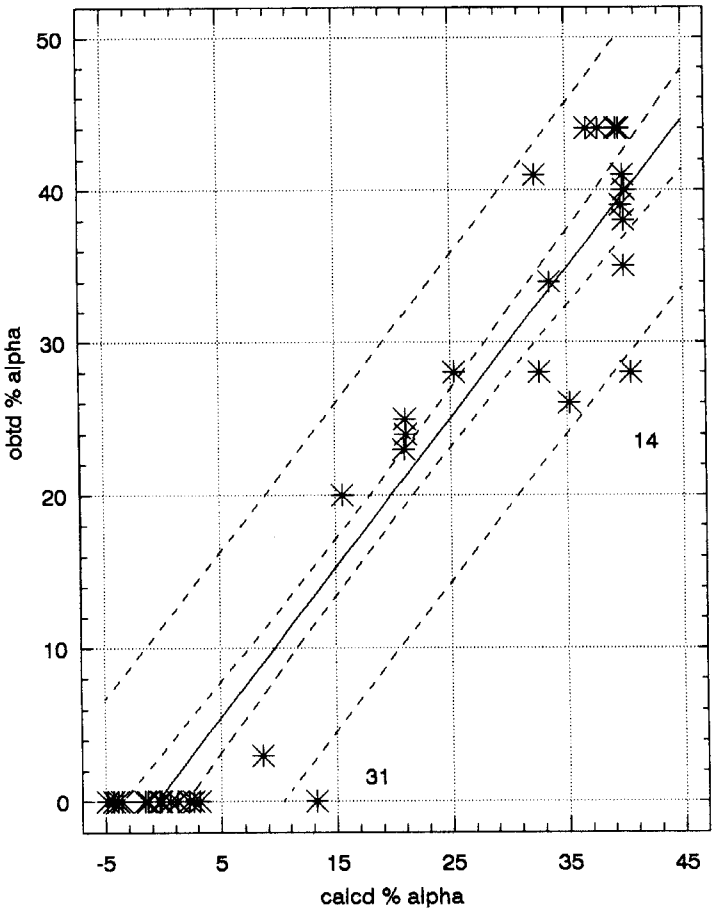

FIGURE 1 Plot of the experimentally obtained *versus* the theoretically calculated percentage of an α-helix conformation of the Aβ(1-42) peptide. The 95% confidence and prediction limits are shown, together with potential outliers marked by their sample number.

Using another backpropagation model which takes less into account the problem of noisy input and noisy output data than the above approach, the squared multiple correlation coefficients were 0.14 (random coil), 0.41 (β-turn), and 0.78 (α-helix, β-sheet).

Using the conventional ordinary least-squares and partial-least squares (two components) regression models, we obtained 0.68 and 0.67 (α-helix), 0.71 and 0.71 (β-sheet), 0.29 and 0.25 (random coil), and 0.79 and 0.78 (β-turn), respectively.

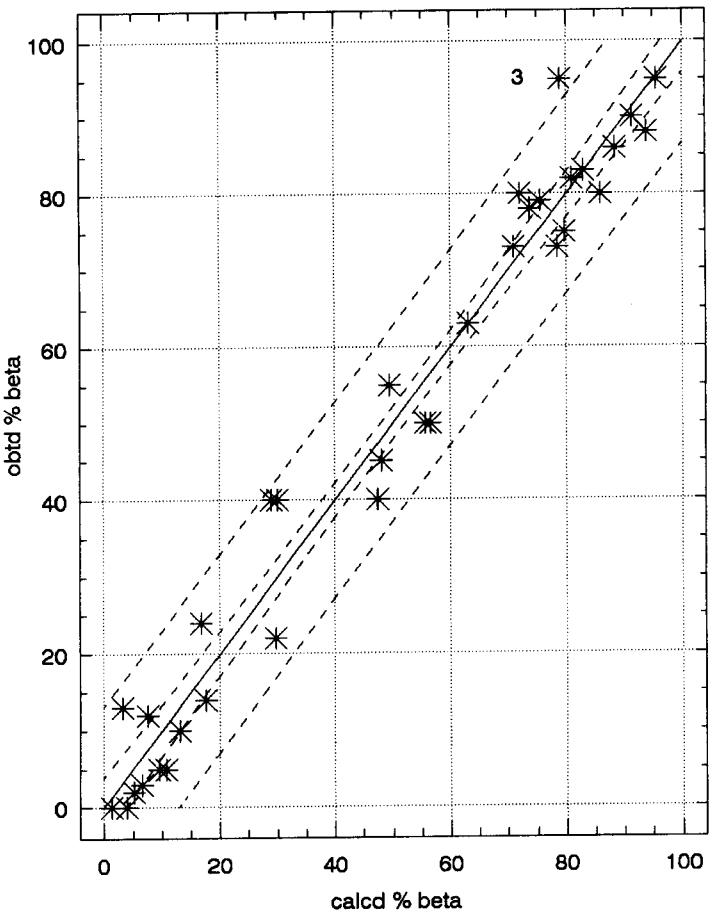

FIGURE 2 Plot of the experimentally obtained *versus* the theoretically calculated percentage of a β-sheet conformation of the Aβ(1-42) peptide. The 95% confidence and prediction limits are shown, together with potential outliers marked by their sample number.

Cross-validation Set of the Backpropagation Neural Network Model

The most effective way of validating a model is to collect fresh data and directly compare the model prediction against them. The "second-best" way is the use of resampling techniques where alternative sequences of submodels are formed to simulate the concept of repeatable experiments. In cross-validation, any subsample taken *randomly* from the *same* "finite population" is used for determining statistical estimators, and the remaining

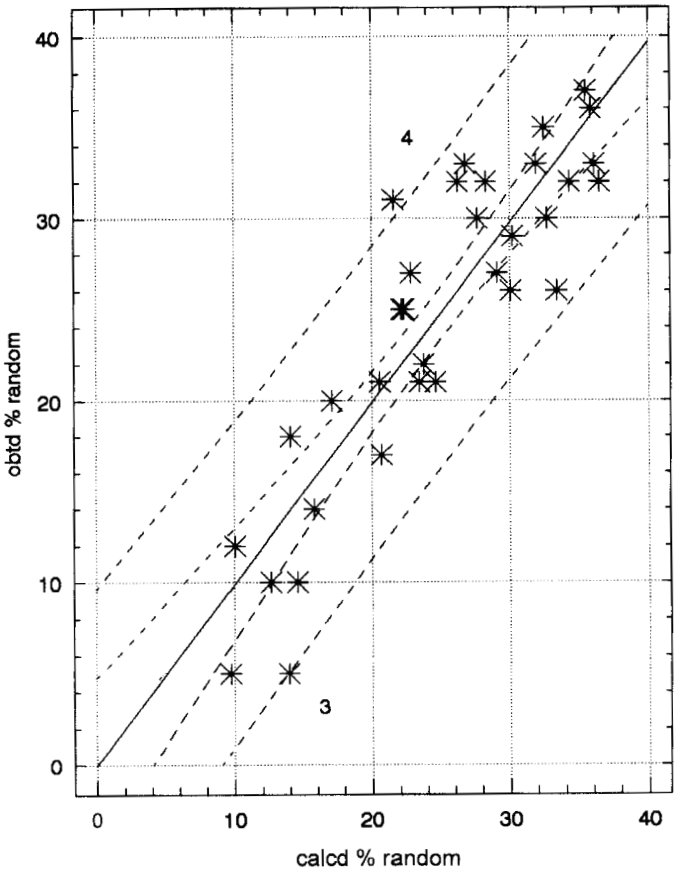

FIGURE 3 Plot of the experimentally obtained *versus* the theoretically calculated percentage of a random-coil conformation of the Aβ(1-42) peptide. The 95% confidence and prediction limits are shown, together with potential outliers marked by their sample number.

subsample is used for testing. There can be no differences between these subsamples other than for sampling errors. This equal distribution of randomly chosen subsamples is the safeguard for generalizability of hypothesis testing and causal inference [12].

The sample was divided randomly into two subsamples of sizes $N_1 = N_2 = 17$. The first subsample is used to get a neural network function which correctly represents those data with which the function was developed (training set). The second subsample was used to test the ability of this function to correctly represent those data that were excluded in the process of derivation of the neural network function (test set).

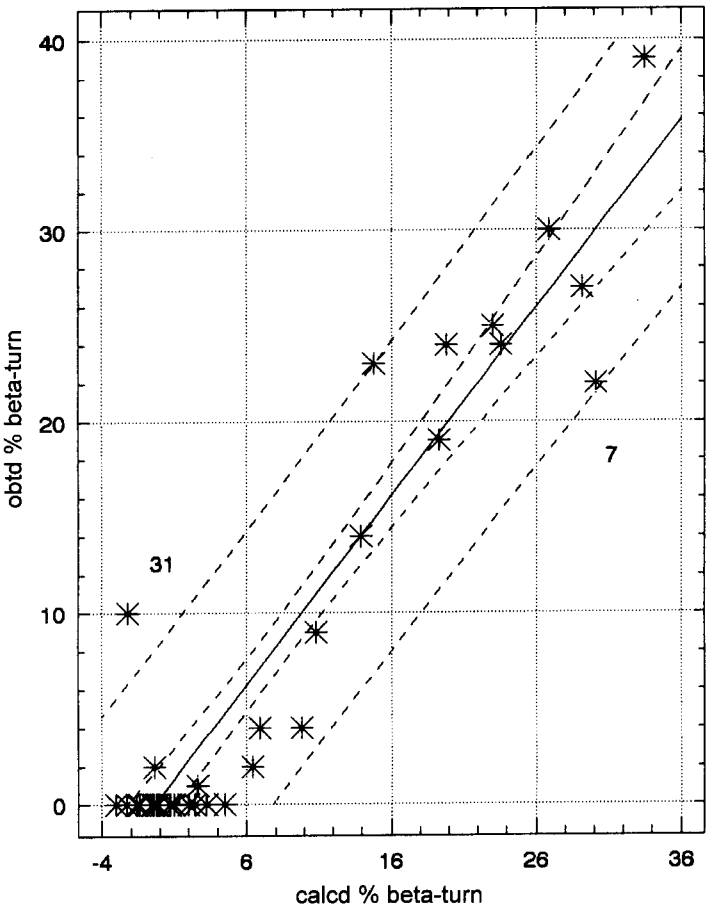

FIGURE 4 Plot of the experimentally obtained *versus* the theoretically calculated percentage of a β-turn conformation of the Aβ(1-42) peptide. The 95% confidence and prediction limits are shown, together with potential outliers marked by their sample number.

TABLE III Results of the cross-validation procedure

Output node	*SD*	*Bias*	*Max. error*	R^2
Training set:				
α-helix	3.94	0.01	6.35	0.976
β-sheet	3.52	0.09	8.98	0.995
Random coil	1.96	0.03	4.30	0.971
β-turn	4.71	−0.11	9.07	0.932
Test set:				
α-helix	8.14	−1.77	17.45	0.893
β-sheet	15.07	−0.67	33.65	0.884
Random coil	6.08	−0.18	13.51	0.773
β-turn	6.40	3.22	15.45	0.791

Table III summarizes the results. Although there are some differences in location (mean values not shown here) and scale (standard deviations, error), it appears that the differences in orientation (correlation) are quite tolerable. This conclusion is supported if the theoretically calculated values are considered (Tab. IV).

Remark Needless to say, negative percentages are physically senseless. They must be considered only in the context of statistically estimated error rates.

TABLE IV Comparison between experimentally obtained (Obtd) and theoretically calculated (Calcd) and predicted (Prdd) conformational states. The experimental error is ± 10%

	α-helix		*β-sheet*		*Coil*		*β-turn*	
Member	*Obtd*	*Calcd*	*Obtd*	*Calcd*	*Obtd*	*Calcd*	*Obtd*	*Calcd*
2	0	−3	88	87	12	12	0	1
5	44	38	5	8	26	29	25	25
6	39	40	2	5	29	29	30	28
7	35	41	13	4	30	26	22	30
8	40	41	0	3	21	22	39	32
9	0	−1	79	79	21	22	0	0
12	3	7	63	64	33	29	1	2
13	26	32	24	18	37	36	30	14
15	38	40	3	6	35	31	24	24
18	24	19	55	53	21	21	0	7
22	44	39	5	8	32	35	19	21
23	0	1	78	76	22	24	0	0
24	0	−2	80	84	20	20	0	−1
26	0	−2	90	86	10	10	0	1
28	0	2	73	75	27	26	0	−1
29	28	24	40	39	30	31	2	8
31	0	6	80	82	10	10	10	1
	Prdd	*Obtd*	*Prdd*	*Obtd*	*Prdd*	*Obtd*	*Prdd*	*Obtd*
1	−6	0	99	86	10	14	−3	0
3	7	0	61	95	19	5	7	0
4	24	20	30	45	25	31	16	4
10	−5	0	93	83	20	17	−3	0
11	−3	0	87	75	23	25	−2	0
14	38	28	9	12	36	36	19	24
16	41	41	5	0	28	32	29	27
17	7	0	69	82	13	18	5	0
19	24	41	41	22	30	33	8	4
20	31	44	25	14	35	33	11	9
21	35	44	15	10	37	32	15	14
25	−3	0	89	95	12	5	−1	0
27	1	0	78	73	19	27	0	0
30	11	25	69	50	18	25	3	0
32	23	23	48	50	22	25	7	2
33	31	28	32	40	29	32	10	0
34	41	34	9	40	37	26	15	0

Prediction Set of the Backpropagation Neural Network Model

Taken the previous results together, there are good reasons to suggest that the neural network functions "work well". This conclusion may lead to an attempt to predict "directly" the influence of solution effects to conformational states, that is, to employ the model to data that were not included in the training and test set. In particular, general solution conditions to form β-sheets should be forecasted.

Table V shows the results. It can be seen that the influence of the pH is negligible if "medically important pH values" were studied (pH 7.4 and 6.6). This is in contrast to the hypothesis that two pH values are of interest in research of Alzheimer's disease: a pH of 7.4 which is found in blood plasma and brain in "normal individuals", and a pH of 6.6 which was found in the brain from patients with Alzheimer disease who died suddenly – compared with the pH 7.1 of patients without Alzheimer's s disease who died suddenly [21].

Also, the influence of relatively low concentrations of the Aβ(1-42) peptide (for example, 1.7 μM) and higher concentrations (for example, 17 μM) is predicted. In water and at low peptide concentrations, the β-sheet conformation dominates. This is consistent with the experimental result that monomeric β-sheets are soluble in water [5], and the hypothesis that small concentrations of the peptide form a soluble nucleating center which goes over after a certain time ("aging") into a supersaturated solution characterized by a spontaneous, slow growth of large, polymeric, unsoluble, neurotoxic aggregates [5, 6, 18]. At higher concentrations, the α-helix and

TABLE V Forecasts of conformational states by using novel and typical solution conditions

Input data			*Predicted output data (percentages)*			
Conc	*% solv.*	*pH*	*α-helix*	*β-sheet*	*Coil*	*β-turn*
17.0	60	7.4	3	95	7	−6
8.3	60	7.4	40	5	30	27
1.7	60	7.4	33	10	19	31
17.0	60	6.6	7	89	11	−5
8.3	60	6.6	40	5	30	28
1.7	60	6.6	35	8	20	32
17.0	0	7.4	39	9	42	10
8.3	0	7.4	11	42	34	12
1.7	0	7.4	−4	83	8	7
17.0	0	6.6	41	5	42	12
8.3	0	6.6	8	49	33	10
1.7	0	6.6	−5	90	6	5

random-coil conformations form a mixture of conformational states, a behavior which is well known from other peptides [13].

Furthermore, the solvents TFE and HFIP promote hydrogen-bonding forces but are weaker proton donors than water, it forces the formation of intramolecular hydrogen bonds. Thus, the effect of a concentration of, say, for example, 60% solvent is of particular interest (Tab. V). As expected, the α-helix and β-turn dominate at low peptide concentrations. The β-sheet conformation dominates at high peptide concentrations and in aqueous solution containing 60% TFE. The reason is probably that a supersaturated solution plus an increase of intramolecular hydrogen bonds stabilizes polymeric β-sheets. Of course, another condition is that the hydrophobic cores of the Aβ(1-42) peptide (Lysl6 to Val18, Lys28 to Val40) are able to interact noncovalently. Consistent with this interpretation is that *equivalent solution conditions* of the Aβ(29-42) segment led to a 60% β-sheet conformation while the Aβ(1-23) segment did not led to a β-sheet state [2]. In the first case, the large lipophilic core Lys28-to-Val40 was present, in the second case, the small lipophilic Lysl6-to-Val18 core was only present. If the complete molecule is analyzed, it might be expected (Tab. V) that the percentage of the β-sheet state increases.

Prediction of Circular Dichroism Spectra

The results direct the attention to a prediction of circular dichroism spectra. First, let us consider the last row of Table V (1.7 μM peptide concentration, water, pH 6.6). There is a β-sheet conformation (90%), as shown by a broad negative band at 217 nm and a positive band at 193 nm, while the absence of any notatable absorptions at 208 nm or 222 nm suggests that little or no α-helix exists (Fig. 5). As second example, the conformation obtained by geometry-optimization of solution NMR data, was used. In this case, a mixture of an α-helix and β-turn might be expected (Fig. 6) because these conformation have the most stable conformers compared with the β-sheet, 3_{10}-helix, double-C7 chair, and so on. The 3D-structure can be downloaded in HyperChem format because this format can be easily converted into SYBYL, ALCHEMY, MOPAC, MOBY, and other file formats of molecular modelling packages. Physicochemical data and the relative energies are listed in this file. Molecular modelling has shown that relatively strong intramolecular hydrogen-bonding forces stabilize the conformation.

The resulting CD spectrum is illustrated by Figure 7. There is an isodichroic range, that is, a "point" where the CD intensities are equal which shows a mixture of two conformational states (50% a-helix, 33%

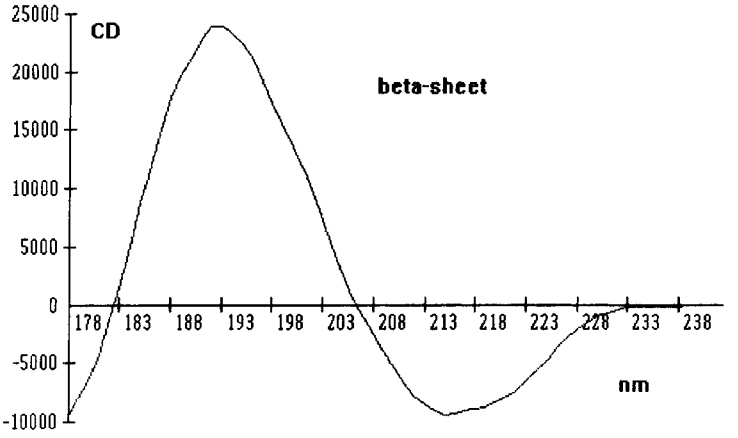

FIGURE 5 Predicted circular dichroism spectrum of a β-sheet conformation of the Aβ(1-42) peptide using a peptide concentration of 1.7 μM, water, and a pH of 6.6 (Tab. V).

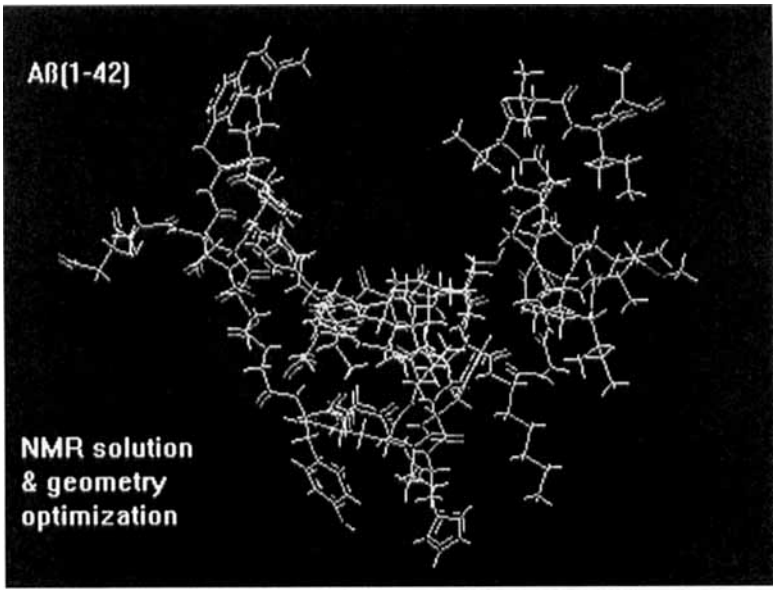

FIGURE 6 Gasteiger-MM+ geometry-optimized conformation of the Aβ(1-42) peptide. The input coordinates of the spatial structure was determined by NMR solution spectroscopy. The optimized molecule can be downloaded from the Internet in order to get a visual impression of the three-dimensional structure (address see text). Colors: green, carbon; red, oxygen; white, hydrogen; blue, nitrogen; yellow, sulfur. The yellow-marked area in the middle is the lipophilic, α-helical, folder region (Leu17 to Ala21) which allows to build the two antiparallel β-sheets of the remaining amino acids. It is the potential receptor site of β-sheet-blocking peptidomimetics. (See Color Plate I).

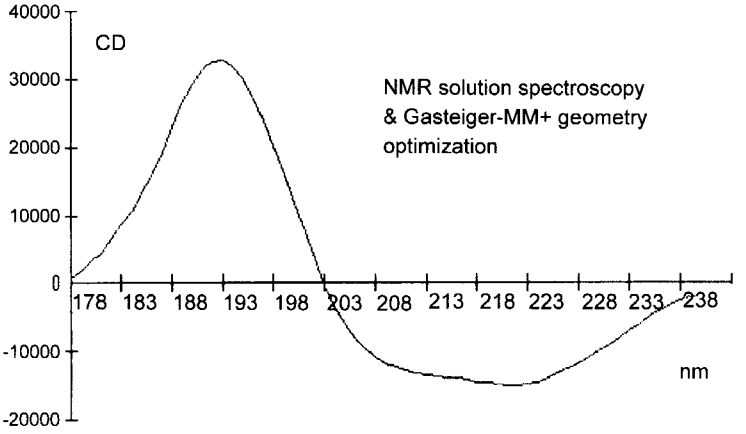

FIGURE 7 Predicted circular dichroism spectrum of the Gasteiger-MM+ geometry-optimized conformation.

β-turn). Using the inverse backpropagation neural network model (exchange of the inputs and outputs), the following environmental conditions were simulated by NMR solution and subsequent geometry-optimization: 15 μM peptide concentration, 35% solvent, pH = 4.27.

It was mentioned that a time-dependent conversion of an untoxic random-coil to a neurotoxic β-sheet of the Aβ(1-42) peptide was found [18].

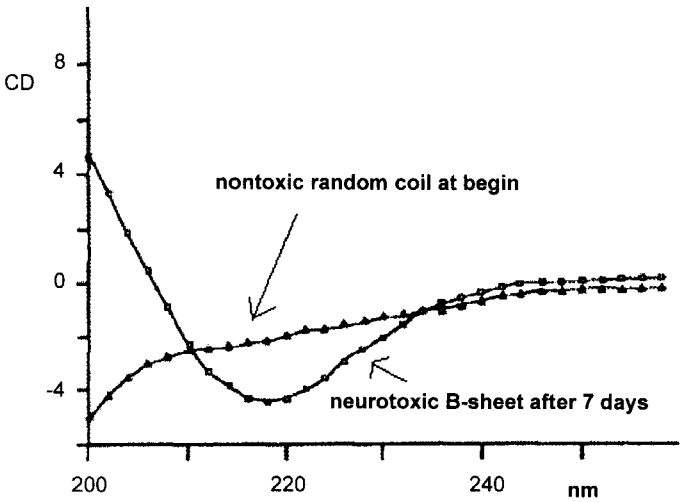

FIGURE 8 Time-dependent transition of a untoxic random-coil (at day 0) to a neurotoxic *b*-sheet conformation (at day 7) of the Aβ(1-42) peptide. Modified after Simmonis *et al.* (1994).

The β-sheet can be shown by a broad negative band at 217 nm (Fig. 8), it agrees with the previous results.

CONCLUSIONS AND FUTURE PERSPECTIVES

Quite recently, time- and solution-dependent transitions were found from untoxic random-coil to neurotoxic β-sheet conformations of the Aβ(1-42) peptide of Alzheimer's disease. To simulate the solution-dependent conformational states of the Aβ(1-42) peptide, an optimized backpropagation neural network model was used. The percentages of the α-helix, β-sheet, random-coil, and β-turn were considered as output parameters, while the concentration of the Aβ(1-42) peptide, the concentration of the solvents trifluoroethanol and hexafluoro-2-propanol, and the pH were defined as input parameters. It was shown that the chosen neural network simulates well the solution-dependent conformations. The result was repeatable by cross-validation where two subsample with equal sizes were randomly chosen, one was used to determine statistical estimators, the other was used for testing. As consequence, solution conditions of a β-sheet conformation of the Aβ(1-42) peptide can be forecasted, or a prediction of circular dichroism spectra is possible. The model was also tested by using the Gasteiger-MM+ geometry-optimized conformation of the Aβ(1-42) peptide where the initial coordinates were obtained by NMR solution spectroscopy.

While aggregation of soluble Aβ(1-42) and Aβ(1-40) peptides into unsoluble oligomers is believed a crucial (but not absolute) determinant in the pathogenesis of Alzheimer's disease, direct or indirect inhibition of the Aß peptide aggregation by drugs appears to be an attractive therapeutic target.

Acknowledgments

I thank for Monika Bretschneider and Rosemarie Wolfram.

APPENDIX: TECHNICAL NOTES

The address is: http://www.uni-leipzig.de/~pharma/ppm2.htm, click on Ref. (207). Table I is available as ASCII file and called CD(1-42). DAT. The geometry-optimized conformation file was called CD(1-42). HIN. It includes the net atomic charges and molecule coordinates of Figure 6,

together with physicochemical informations and the relative energies of the "most stable" conformer. The multivariate regression (MASCA) can be downloaded, too (self-extracting zipped file).

References

[1] Allinger, N. L. and Yan, L. (1993). Molecular mechanics (MM3). Calculation of furan, vinyl, ethers and related compounds, *J. Am. Chem. Soc.*, **115**, 11918–11925.

[2] Barrow, C. J., Kenny, P. T. M., Ykikazu, M. and Zagorski, M. G. (1992). Solution conformations and aggregational properties of synthetic amyloid β-peptides of Alzheimer's disease, *J. Mol. Biol.*, **225**, 1075–1093.

[3] Frey, R. F., Cheng, V. K. W., Coffin, J., Momany, F. A., Newton, S. Q., Ramek, M. and Schäfer, L. (1992). Importance of correlation-gradient geometry optimization for molecular conformational analyses, *J. Am. Chem. Soc.*, **114**, 5369–5377.

[4] Gasteiger, J. and Marsili, M. (1980). Iterative partial equalization of orbital electronegativity – a rapid access to atomic charges, *Tetrahedron*, **36**, 3219–3288.

[5] Hilbich, C., Beyreuther, K., Hilbich, C., Kisters-Wolke, B., Masters, C. L. and Reed, J. (1991). Aggregation and secondary structure of synthetic amyloid βA4 peptide of Alzheimer's disease, *J. Mol. Biol.*, **218**, 149–163.

[6] Jarrett, J. T., Berger, E. B. and Lansburg, P. T. Jr. (1993). The carboxy terminus of the β amyloid protein is critical for the seeding of amyloid formation: implications for the pathogenesis of Alzheimer's disease, *Biochemistry*, **32**, 4693–4697.

[7] Kanô, F. and Maeda, H. (1984). Monte Carlo Simulation of the β-Sheet-Random Coil Transition of a Homopolypeptide, I. Equilibrium Study. *Mol. Simul.*, **16**, 261–274.

[8] Kemp, D. S., Allen, T. J. and Ostlick, S. L. (1995). The energetics of helix formation by short-peptides in aqueous solution. 1. Characterization of the reporting helical template Ac-Hel_1, *J. Am. Chem. Soc.*, **117**, 6641–6657.

[9] Kraft, G. (1994). Perspectives on amyloid and Alzheimer's disease: a critical review, *Ann. Rep. Med. Chem.*, **28**, 49–58.

[10] Maeda, H., Gatto, Y. and Ikeda, S. (1984). Effects of chain length and concentration of the β-coil conversion of poly[S-carboxymethyl-L-cysteine] in 50 nM NaCl solution, *Macromolecules*, **17**, 2031–2037.

[11] Mager, P. P. (1991). *Design Statistics in Pharmacochemistry*, Wiley, New York, p. 174.

[12] Mager, P. P. (1996). A random number experiment to simulate resample model evaluations, *J. Chemometrics*, **10**, 221–240.

[13] Mager, P. P. (1997). Multivariate investigations of random-coil and ordered-structure conformations of the Tyr181-to-Tyr188 segment of HIV-1 reverse transcriptase, *Mol. Simulation*, **19**, 17–41.

[14] Mori, H., Ogawara, M., Selkoe, D. J. and Takio, K. (1992). Mass spectrometry of purified amyloid β protein in Alzheimer's disease, *Biol. Chem.*, **267**, 17082–17806.

[15] Prelli, F., Bots, G. T. A. M., Castano, E. M., van Duinen, S. G., Frangione, B. and Luyendijk, W. (1988). Differential processing of Alzheimer's β-protein precursor in the vessel wall of patients with hereditary cerebral hemorrhage with amyloidosis-Dutch type, *Biochem. Biophys. Res. Commun.*, **151**, 1150–1155.

[16] Sreerama, N. and Woodey, W. W. (1993). A self-consistent method for the analysis of protein secondary structure from circular dichroism, *Anal. Biochem.*, **209**, 32–44.

[17] Selkoe, D. J. (1994). Normal and abnormal biology of the β-amyloid precursor protein, *Ann. Rev. Neurosci.*, **17**, 489–517.

[18] Simmonis, L. W., Becker, G. W., Brems, D. N., Brigham, E. F., Fuson, K. S., Li, W. Y., Lieberburg, I., May, P. C., Reydel, R. E., Tomaselli, K. J. and Wright, S. (1994). Secondary structure of amyloid β peptide correlates with neurotoxic activity *in vitro*, *Mol. Pharmacol.*, **45**, 373–379.

[19] Tai, J. C., Allinger, N. L. and Yang, L. (1993). Molecular mechanics (MM3) calculation on nitrogen-containing aromatic heterocyclics, *J. Am. Chem. Soc.*, **115**, 11906–11917.

[20] Williams, M., Puttfarcken, P. and Shiosaki, K. (1995). Amyloid β peptide in Alzheimer's disease pathology: towards a rational basis for drug discovery? *Exp. Opin. Invest. Drugs*, **4**, 263–270.
[21] Yates, C. M., Butterworth, J., Gordon, A. and Tennant, M. C. (1990). Enzyme activation in relation to pH and lactate in postmortem brain in Alzheimer-type and other dementias, *J. Neurochem.*, **55**, 1624–1630.
[22] Zupan, J. and Gasteiger, J. (1993). *Neural Networks for Chemists*, VCH, Weinheim.